

Multiplexed Signal Ion Emission Reactive Release Amplification (SIERRA) Assay for the Culture-Free Detection of Gram-Negative and Gram-Positive Bacteria and Antimicrobial Resistance Genes

Michael Pugia, Tiyash Bose, Marco Tjioe, Dylan Frabutt, Zane Baird, Zehui Cao, Anna Vorsilak, Ian McLuckey, M. Regina Barron, Monica Barron, Gerald Denys, Jessica Carpenter, Amitava Das, Karamjeet Kaur, Sashwati Roy, Chandan K. Sen, and Frédérique Deiss*



Cite This: *Anal. Chem.* 2021, 93, 6604–6612



Read Online

ACCESS |



Metrics & More

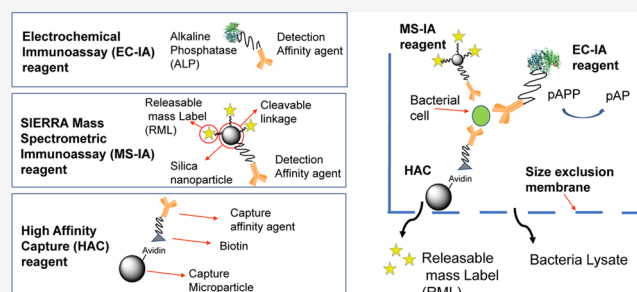


Article Recommendations



Supporting Information

ABSTRACT: The global prevalence of antibiotic-resistant bacteria has increased the risk of dangerous infections, requiring rapid diagnosis and treatment. The standard method for diagnosis of bacterial infections remains dependent on slow culture-based methods, carried out in central laboratories, not easily extensible to rapid identification of organisms, and thus not optimal for timely treatments at the point-of-care (POC). Here, we demonstrate rapid detection of bacteria by combining electrochemical immunoassays (EC-IA) for pathogen identification with confirmatory quantitative mass spectral immunoassays (MS-IA) based on signal ion emission reactive release amplification (SIERRA) nanoparticles with unique mass labels. This diagnostic method uses compatible reagents for all involved assays and standard fluidics for automatic sample preparation at POC. EC-IA, based on alkaline phosphatase-conjugated pathogen-specific antibodies, quantified down to 10^4 bacteria per sample when testing *Staphylococcus aureus*, *Escherichia coli*, and *Pseudomonas aeruginosa* lysates. EC-IA quantitation was also obtained for wound samples. The MS-IA using nanoparticles against *S. aureus*, *E. coli*, *Klebsiella pneumoniae*, and *P. aeruginosa* allowed selective quantitation of $\sim 10^5$ bacteria per sample. This method preserves bacterial cells allowing extraction and amplification of 16S ribosomal RNA genes and antibiotic resistance genes, as was demonstrated through identification and quantitation of two strains of *E. coli*, resistant and nonresistant due to β -lactamase cefotaximase genes. Finally, the combined immunoassays were compared against culture using remnant deidentified patient urine samples. The sensitivities for these immunoassays were 83, 95, and 92% for the prediction of *S. aureus*, *P. aeruginosa*, and *E. coli* or *K. pneumoniae* positive culture, respectively, while specificities were 85, 92, and 97%. The diagnostic platform presented here with fluidics and combined immunoassays allows for pathogen isolation within 5 min and identification in as little as 15 min to 1 h, to help guide the decision for additional testing, optimally only on positive samples, such as multiplexed or resistance gene assays (6 h).



More than 2.8 million antibiotic-resistant infections occur in the United States each year and more than 35 000 people die as a result.¹ Diabetic patients are an immunocompromised population at particular risk of poor outcomes, as their macrophages become deficient in phagocytosis impairing their ability to clear microbial pathogens from chronic wounds, urinary tract, and respiratory infections.^{2–10} This impairment makes treatment more difficult and increases the vulnerability to infections by antibiotic-resistant bacteria such as *Staphylococcus aureus*, *Acinetobacter baumannii*, *Klebsiella pneumoniae*, *Pseudomonas aeruginosa*, and *Escherichia coli*.

The standards of care for detecting Gram-positive and Gram-negative pathogens use culturing to detect bacteria at densities exceeding 10^5 cells/mL in their planktonic form.¹¹ Culturing is not easily extensible to the rapid identification of organisms and is not timely for deciding treatments at the

point-of-care (POC).¹² Furthermore, the CDC estimates that 65% of all human infections are caused by biofilm-forming bacteria, whereas the National Institutes of Health estimates a number closer to 80%.¹³

Additionally, culture-dependent diagnostic methods cannot detect biofilms, thus grossly underestimating the severity of infections, which leads to poor therapeutic outcomes.^{14,15} Detection of metabolites produced by film-forming bacteria, such as pyrocyanine from *P. aeruginosa*, is possible but requires

Received: January 31, 2020

Accepted: March 17, 2021

Published: April 5, 2021



lengthy sample processing.^{16,17} Therefore, POC diagnostic assays that can detect both planktonic and biofilms pathogens are urgently needed. Such technologies must be able to detect the presence of microbes regardless of their colony-forming ability, and in much shorter timescales than culture-dependent methods, ideally within 15 min.

Diagnostic methods utilizing antibodies raised against antigens from cell lysates recognizing specific membrane components can identify particular bacterial species. For example, antibodies can be designed to target the adhesins, teichoic acid of *S. aureus*, O-antigen lipopolysaccharides of *E. coli*, or the O-antigen polysaccharides of *P. aeruginosa* and *K. pneumoniae* among others.^{18–22} The immunoassays can be utilized by flow cytometry, immunochromatography, or enzyme-linked immunosorbent assays (ELISA) to measure bacteria, but they are not sensitive below 10⁶ bacteria/mL.^{23–26} The 16S rRNA gene is highly conserved among bacteria²⁷ and has been used for phylogenetic analysis,²⁸ prediction of culture results,²⁹ and assessment of infections.^{29,30} It contains sequences that are similar in all bacteria, allowing the use of a universal primer set,³¹ as well as variable sequences that distinguish individual species; however, current assays for the 16S gene do not meet the requirements for a rapid test.

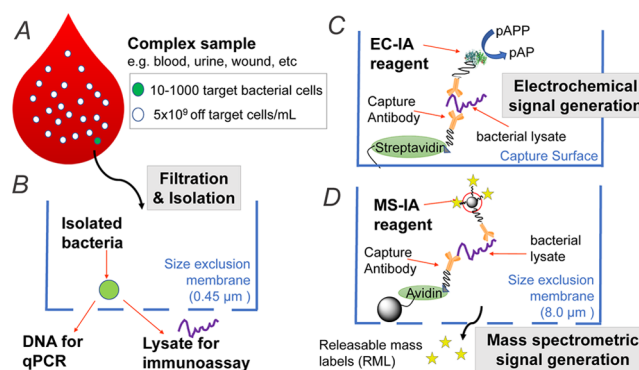
Advances in nanotechnology have increased the sensitivity of immunoassays, making single-cell detection a feasible goal; however, the integration has required parallel advances in microfluidics for POC sample preparation.^{32,33} The key technical limitation of current approaches has been the lack of rapid isolation integrated with affinity binding methods for the culture-free detection of small numbers of bacteria (~10⁴ cells/mL) in complex samples, which is needed for the immediate selection and initiation of appropriate treatments.³³ Furthermore, antibiotic stewardship requires rapid (<60 min) confirmation of pathogen positives in the clinical microbiology laboratory using highly multiplexed and quantitative enumeration and distinction of molecular differences in pathogens. Nanoparticles have been used to develop electrochemical immunoassays (EC-IAs) for POC hand-held analyzers, with sufficient sensitivity to detect 10 bacterial cells in buffer.^{34,35} Clinical assays would however require further reduction of sample interference by fluidics for automatic sample preparation, the ability to detect multiple bacterial species in parallel, and the ability to quantitate cell counts across several orders of magnitude to maintain the cost-reducing advantages of POC testing.³⁶

We recently demonstrated highly sensitive mass spectral immunoassays (MS-IAs) based on nanoparticles incorporating signal ion emission reactive release amplification (SIERRA) technology using antibodies for the detection of Her2/neu⁺ cancer cells in whole blood, combined with the same-sample analysis of cancer cell mRNA.³⁷ This achieved a 1000-fold increase in sensitivity, needed for culture-free methods when compared to chemiluminescent immunoassays, with a limit of detection (LOD) of ~20 cells. This was achieved using carnitine-labeled pentapeptides as releasable mass labels (RMLs) bound to nanoparticles by cleavable –S–S– linkages, combined with the rapid size-exclusion fluidics for automatic sample preparation. While amendable to laboratory testing, the MS-IA time to results is not in line with POC timescales and requires relatively high concentrations of TCEP or DTT to release mass labels for

detection, which suppresses the MS signal and detracts from sensitivity.

Here, we set out to demonstrate the rapid high sensitivity detection of bacteria by a combination of EC-IA and MS-IA performed with compatible reagents and using the same size-exclusion standard fluidics for automatic sample preparation in a rapid POC analysis format. A sample (blood, urine, wound) was filtered on a membrane and then lysed to generate isolated aliquots for subsequent assays (Scheme 1A,B). EC-IA is performed using alkaline phosphatase (ALP)-

Scheme 1. Methodology Utilized^a



^aBacteria from a complex sample (A) are isolated by size-exclusion filtration (B) and lysed to collect aliquots for the immunoassays and DNA assays (B). Lysates are subsequently used for electrochemical immunoassays (EC-IA) using high-affinity capture surfaces (C) and for mass spectrometric immunoassays (MS-IA) using high-affinity capture microparticles and size-exclusion filtration (D).

conjugated pathogen-specific antibodies to generate a fast and sensitive electrochemical response (Scheme 1C). A confirmatory multiplexed enumeration by MS-IA is then performed using pathogen-specific antibodies linked to SIERRA nanoparticles decorated with unique mass labels detectable through new rapid release –C–O– linkage chemistry (Scheme 1D). We also verified the compatibility of this rapid bacterial capture method as a DNA isolation method for quantitative polymerase chain reaction (qPCR) analysis of antimicrobial resistance and 16S ribosomal RNA (rRNA) as an additional, downstream, confirmatory method.

This novel combination of assays and the microfluidic isolation method offers selective sample processing for bacterial immunoassay for both POC and laboratory settings, to increase the speed and accuracy needed for rapid diagnosis and treatment of resistant infection.

MATERIALS AND METHODS

Reagents and Equipment. For MS analysis, we used an LTQ-XL linear ion trap mass spectrometer (Thermo Fisher Scientific, Waltham, MA) fitted with a Dionex Ultimate 3000 autosampler. The mass label peptides betaine-Ala-Val-Ile-Val-Ala (AA-5), betaine-Val-Val-Val-Gly-Val (VV-5), betaine-Ile-Ile-Val-Ala-Gly (IG-5), betaine-Gly-Gly-Gly-Lys-Lys (GL-5), betaine-Val-Gly-Ile-Al-Ile (VI-5), carnitine-Ala-Ala-Val-Iso-Cys (AC-5), and carnitine-Ala-Iso-Ala-Val-Cys (AC-5.2) were supplied at >95% purity by Celtek (Franklin, TN). For EC analysis, we used screen-printed gold electrodes in a 96-well format (DRF 220–96, Metrohm USA, Riverside, FL) using the μ STAT 8000 potentiostat (Metrohm). For qPCR, we used the QuantStudio 3 instrument (Applied

Biosystems, Carlsbad, CA) using QuantStudio Design & Analysis Software. Standard laboratory reagents were obtained from Thermo Fisher Scientific unless otherwise stated.

Clinical Specimens. Urine ($n = 228$) and wound ($n = 37$) specimens were obtained from patients undergoing assessment of urinary tract infections or wound therapy as part of standards of care at the IU Health University Hospital and The Ohio State University Comprehensive Wound Center, respectively. Complete culture results were obtained for all samples. A positive result was indicated with 5×10^4 cells/mL by culture using hospital standard operating procedures.

Wound specimens were collected from dressings (sponges) as patients presented for care with fluid and cells released by lavage with saline solution and frozen at -80 °C until tested.^{14,15} Specimens were thawed at room temperature before testing and prepared for lysate analysis by diluted 1:1 in phosphate-buffered saline (PBS) and sonicated using a Q500 device with a cup-horn attachment (Qsonica, Hartford, CT) at 4 °C. Sonication at 88% amplitude was carried out for 45 min in total (3 s pulses with 3 s gaps, 22.5 min of sonication). The protein concentration was determined using a Pierce BCA protein quantification kit (Thermo Fisher Scientific) and samples were restored in aliquots at -80 °C until analyzed.

Urine samples were selected based on distribution of gram (–) and (+) species by culture and stored immediately at -80 °C until analyzed. Specimens with multiple organisms in culture ($n = 23$) were flagged as potentially contaminated or excessive sedimentation upon thawing ($n = 36$) and excluded from further analysis. Extended-spectrum β -lactamase resistance (ESBL) was identified by minimal inhibitor concentrations (MIC) from antibiotic susceptibility testing ($n = 9$).

All human studies were approved by the Institutional Review Board following written informed consent provided by the enrollees. A double-blind process was used for testing, according to the Declaration of Helsinki protocols. All specimens were stored at -80 °C following collection.

Preparation of Microorganism Testing Standards.

Pseudomonas aeruginosa (ATCC 27853), *Escherichia coli* (ATCC 25922, AR-Bank no. 0077 and no. 0086), *Staphylococcus aureus* (ATCC 27661), and *Klebsiella pneumoniae* (ATCC 13883) bacterial stocks were generated and maintained by standard microbiologic culture practices (Supporting Information 1). The lysed samples were prepared from bacterial stocks (10^8 cells/mL) resuspended in radioimmunoprecipitation assay (RIPA) buffer (Alfa Aesar, Ward Hill, MA) containing Pierce protease inhibitor (Thermo Fisher Scientific) and were sonicated as described above for specimens. The sonicated *P. aeruginosa*, *E. coli*, *S. aureus*, and *K. pneumoniae* samples were diluted 1:10 in RIPA buffer with protease inhibitor and sonicated again as above. Standards of 10^7 cells/mL based on original McFarland counts were prepared before sonication. Protein concentration was measured using the Pierce BCA assay to determine the protein released from 10^7 bacteria. Protein concentration was 20 ng protein per 10^6 Gram-positive *S. aureus* and ranged 40–50 ng protein per 10^6 for all Gram-negative species tested. Three serial dilutions (1:10) with 1% bovine serum albumin (BSA) in PBS were prepared as additional standards at 10^6 , 10^5 , and 10^4 cells/mL as well as a negative control with no cells.

Preparation of Bacterial Affinity Agents. Commercial rabbit polyclonal antibodies against key Gram-positive (*S. aureus*) and Gram-negative (*E. coli*, *K. pneumoniae*, and *P. aeruginosa*) bacteria were selected by cross-reactivity screening using ELISA and fluorescence-activated cell sorting (FACS) analysis of $>10^7$ intact bacteria/mL (Supporting Information 2). Screening identified polyclonal antibodies recognizing *S. aureus* (Thermo Fisher Scientific), *E. coli* (MyBioSource, San Diego, CA), *K. pneumoniae* (Thermo Fisher Scientific), and *P. aeruginosa* (Abcam, Cambridge, U.K.). These were separately conjugated to ALP (Thermo Fisher Scientific) using the FastLink ALP kit (Abnova, Taipei City, Taiwan), to biotin-PEG4 and to Dylight 488 using the EZ-Link NHS-conjugation kits (Thermo Fisher Scientific). Antibody conjugates were stored at 4 °C.

Nanoparticle Reagent Preparation. SIERRA nanoparticles with –C–O– or –S–S– cleavable linkages were prepared using multistep conjugation processes (Supporting Information 3). For both types of particles, the polyclonal antibodies for bacterial detection were bound to the end of a fraction of the poly(ethylene glycol) (PEG) linker. The resulting nanoparticles were characterized (Supporting Information 4) and contained 2000–4500 unique RMLs for each nanoparticle assigned to a unique polyclonal antibody (~ 35 per particle). The nanoparticles were sonicated before use for 5 min at 50% amplitude in 3 s pulses with 3 s gaps.

Bacterial Size-Exclusion Isolation. Membranes and capture particles were first blocked for 1 h with 10% casein, 125 mM MOPSO, 0.2 mM BSA, 0.01 mM hulgG, and Cohn's fraction IV in water adjusted to pH 7.5 for 1 h at RT followed by washing twice with PBS. For intact bacteria, samples (up to 900 μ L) with intact bacteria (1×10^3 – 1×10^7 cells/mL) were isolated by filtration through size-exclusion using 0.45 μ m poly(vinylidene difluoride) (PVDF) membrane in a 96-well (Multiscreen HTS HA Filter Plate, Millipore-Sigma, Burlington, MA). For affinity capture of bacterial lysate or cells, 100 μ L of the block streptavidin microparticles (18.1 μ m in diameter, 1%, Spherotech, Lake Forest, IL) were isolated by filtration through size-exclusion using polycarbonate track-etched size-exclusion filtration membranes (8.0 μ m pore size) in a previously described 96-well fluidic filtration format that was injection molded (Supporting Information 5, Figure S3).³⁷ A vacuum was applied for 30 s to remove the filtrate from the samples followed by rinsing several times with 200 μ L of PBS. Lysates were removed by adding 200 μ L of BPERII (Bacterial Protein Extraction Reagent 2X, Thermo Fisher) to release the lysates for analysis, which were gathered by centrifugation into a receiving plate at 1000g for 1 min at 25 °C to collect the released lysates. Bacteria capture and release was characterized by plating the filtrate and colony-forming unit (CFU) count (Supporting Information 6). Complete isolation of intact cells and lysis was demonstrated.

Bacterial Immunoassay Method. For sandwich immunoassays measured optically or electrochemically, 48 μ L of the biotinylated *S. aureus*, *E. coli*, *K. pneumoniae*, or *P. aeruginosa* polyclonal antibodies (0.75 μ g/assay) and 30 μ L of the same polyclonal antibodies conjugated to ALP (1.50 μ g/assay) (Scheme 1C) were added to 100 μ L of the lysate sample or calibrators with 0, 5, 10, 20, 30, and 40 thousand cells or lysate equivalent per assay and sealed in a polypropylene 96-well sample plate. For MS-IA analysis, 30 μ L of the same polyclonal antibodies conjugated to 100 μ g/

mL NPs with corresponding RML were added in place or addition to the antibodies conjugated to ALP (Scheme 1D). Duplicate samples and controls were incubated on a plate shaker at 35 °C, 800 rpm, for 1 h. To test for sample matrix effects and cross reactivity, sonicated specimens negative for bacteria were spiked with *P. aeruginosa*, *E. coli*, *S. aureus*, and *K. pneumoniae* lysate equivalent to 10^6 , 10^5 , or 10^4 cells/mL compared to negative control. Streptavidin-coated high binding capacity microplates (Pierce) were blocked for 24 h at 4 °C with the blocking agent described above and washed five times with 200 μ L of TBS-T (0.05% Tween-20) (EL406 plate washer, BioTek). Affinity bound samples were transferred and incubated 10 min at 25 °C, and the wells washed five times with 200 μ L of TBS-T. For optical analysis, samples were measured by the absorbance at 405 nm produced by adding 90 μ L of PNPP (substrate tablets dissolved in 100 mM Tris buffer, 600 mM NaCl, and 5 μ M MgCl adjusted to pH 9.0 at 15 min using the Synergy HTX plate reader).

Electrochemical (EC) Detection Method. For EC analysis, a 1.05 mM solution of *p*-aminophenyl phosphate (pAPP, 3.0 mg, MW 189) was prepared fresh each day in 100 mM Tris, 600 mM NaCl, and 5 μ M MgCl₂ adjusted to pH 9.0. A 150 μ L volume of the pAPP solution was added to each well of the reacted bacterial immunoassay plates. Aliquots of 100 μ L were collected after 5 min of reaction with ALP and transferred to sample well containing screen-printed gold electrodes in a 96-well format to obtain electrochemical readings for interday sample replicates ($n = 2$) using separate sensors ($n = 2$ per replicate) by square wave voltammetry (SWV) to take replicate readings ($n = 3$) for each well every 5 min for 30 min. A calibration curve from 500, 400, 300, 100, 50, and 0 pM ALP was prepared and measured for each plate. High and low controls containing 333 and 33 pM of ALP produced average current changes of 2.6 and 0.8 μ A, respectively, at 0.03V (Supporting Information 7).

MS–MS Detection of Mass Labels. For MS–MS analysis of order-adjusted isobaric RML amino acid sequences and internal standards from the same mass-to-charge ratio (m/z) parent, a release from SIERRA nanoparticles was performed (Supporting Information 8). For SIERRA nanoparticles that utilize –C–O– cleavable linkages, 100 μ L of 0.001% citrate release buffer (pH 5.2) containing 52.6 nM IV-5 internal standard was added to the feed side (upstream) of the membrane filter for immediate RML release. For nanoparticles utilizing –S–S– cleavable linkages, 100 μ L of 5 mM TCEP mixed with 25 nM AC-5.2 internal standard in 10 mM ammonium acetate (pH 5.5) was added for release after 30 min of incubation. The plate was centrifuged at 1000g for 1 min at 25 °C to collect released mass labels as previously described.³⁷ For C–O nanoparticle, calibration solutions containing either AA-5, VV-5, IG-5, or GL-5 at 52.6, 26.3, 13.15, 6.58, 3.29, and 1.644 nM with 52.6 nM for VI-5 internal standard for all were prepared in 10 mM ammonium acetate pH 5.5 buffer with 1:1 methanol. For S–S nanoparticle, the calibration solutions contained AC-5 across the sample levels with 25 nM for AC-5.2 internal standard. Blank solutions were also prepared in the same buffer with 52.6 nM VI-5 or 25 nM for AC-5.2 internal standards. The released solution was collected in a fresh 96-well polypropylene sample collection plate by centrifuging at 200g for 2 min as previously described.³⁷ The RML signals in

the calibration solutions and samples were measured by MS/MS in centroid mode. MS/MS scans were used to monitor unique fragments for RML and internal standards to determine the mass label concentrations and correlate them to the number of bacterial cells using calibration curves (Supporting Information 8).

Molecular Analysis of Bacteria. Bacterial 16S rRNA genes and the extended-spectrum β -lactamase resistance gene *CTX-M* were detected by quantitative PCR (qPCR) with TaqMan labile probes. For the 16S rRNA gene, we used forward primer 5'-GGA TTA GAT ACC CBD GTA GTC-3', reverse primer 5'-GGG TYK CGC TCG TTR-3', and the probe 5'-/HEX/CAC GAG CTG ACG ACR RCC ATG CA/Iowa Black quencher/-3'. For the *CTX-M* gene, we used forward primer 5'-GBG ATA ARA CCG GCA GC-3', reverse primer 5'-TGG GTR AAR TAR GTS ACC AG-3', and the probe 5'-/FAM/ACS AAY GAT ATC GCG GTK ATC TGG CC/Iowa Black quencher/-3'. Each 20 μ L reaction contained 10 μ L 2 \times PrimeTime mix (Integrated DNA Technologies, Skokie, IL), 0.4 μ M of each primer, 0.2 μ M of the dye and quencher labeled probe, 1 mg/mL BSA, and 2 μ L of the bacterial lysate as a template. For qPCR, the initial sample heating to 95 °C for 3 min followed by up to 55 cycles of 95 °C for 15 s and 60 °C for 30 s. The products were cooled to 4 °C before threshold count (C_t) analysis. The 16S rRNA amplification products from both *E. coli* strains were able to Sanger sequenced and mapped to known *E. coli* strains using BLAST (Supporting Information 9).

RESULTS AND DISCUSSION

As described in Scheme 1, the main steps of the diagnostic platform are to (i) isolate intact bacteria from complex samples such as urine, wound samples, or treated whole blood and lyse them (ii) collect the lysate in aliquots for subsequent immunoassays and DNA assays, (iii) quickly generate an electrochemical signal via the EC-IA for the detection and quantification of bacteria, (iv) if the EC-IA was positive, perform the confirmatory MS-IA, and (v) if MS-IA is positive, analyze sample further by qPCR DNA for antimicrobial resistance.

Bacterial Isolation. Size-exclusion filtration by PVDF membranes with a pore size of $\leq 0.45 \mu$ m and sufficient membrane area (380 mm²) were highly efficient at isolating intact bacteria cells for up to 0.9 mL of complex samples at a low vacuum (<100 mbar). The counting of *E. coli* and *S. aureus* colonies was performed at each step of the filtration (Supporting information 6, Figure S4). Antigens and DNA were able to be completely recovered by lysis with BPEP-II surfactant by centrifugation for removal from membrane without interference to a separate immunoassay and qPCR analysis, as demonstrated in the ensuing sections. These small-pore membranes could, however, not be used to achieve the limit of quantitation (LOQ) required for culture-free detection as they prevented the passage of immunoassay reagents including nanoparticles, ALP, and pAb-ALP (Supporting Information 6). Size-exclusion filtration using affinity capture by microparticles of 18 μ m diameters by track-etched membranes with 8.0 μ m diameter pores (Figure S5) retained the advantages of capturing bacterial cells from complex samples, and also allowed complete passage of unbound immunoassay reagents as long as the porosity was sufficiently permeable (10^3 pores/mm²) to unbound sample debris.

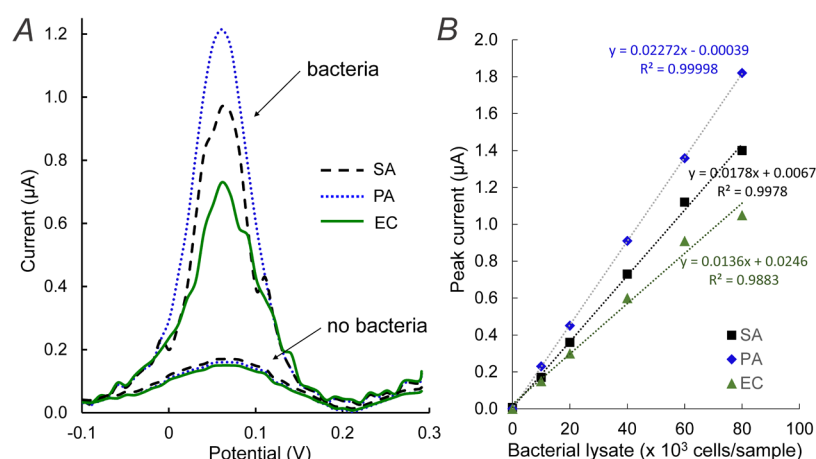


Figure 1. Bacterial immunoassay results. (A) Representative square wave voltammograms (SWV) for EC-IA of the high-affinity sandwich immunoassay response for *S. aureus* (SA), *E. coli* (EC), and *P. aeruginosa* (PA) lysates bound to polyclonal antibodies with biotin and alkaline phosphatase (ALP). (B) Electrochemical calibration curves generated after baseline correction for *S. aureus* (SA), *E. coli* (EC), and *P. aeruginosa* (PA) lysates.

The EC-IA did not require an additional filtration and could be performed with sandwich assays followed by signal measurement on electrodes. Herein, they were performed with high-affinity capture plates. We found no electrochemical background signals from ALP-conjugated antibacterial antibodies or RML signals from SIERRA nanoparticles. Bacterial lysate could be captured selectively for specific cell types. Bacterial genes could be accessed using surfactant lysis to remove DNA from intact cells as shown in the qPCR analysis.

Bacterial Immunoassay. Previously, we showed that polyclonal antibodies against *E. coli* lysate bound multiple epitopes and were suitable for sandwich assays.³³ In agreement, we confirmed that these new polyclonal antibodies raised against lysates also worked in sandwich formats by ELISA and FACS with intact cells, and ELISA with lysates (Supporting Information 2). Sandwich assays were ~100-fold more responsive to lysates than intact cells, as expected due to the release of intracellular antigens. All high-affinity capture immunoassays demonstrated linear responses and achieved an optical LOQ of 10^4 bacteria per sample (Figure S2). The polyclonal assays demonstrated expected selectivity for *S. aureus*, *E. coli*, and *P. aeruginosa* in lysate standards. The nonselectivity observed in screening methods was eliminated in the stronger washing allowed by high-affinity capture format. However, the *K. pneumoniae* antibody remained nonselective (Figure S1A) and was not carried forward to clinical sample testing. Finally, the three immunoassays were tested with optical measurements of wound samples ($n = 37$) as examples of complex-matrix samples. The wound specimens consisted of fluid and cells collected from dressings of patients. All three immunoassays demonstrated quantitation of *S. aureus*, *E. coli*, and *P. aeruginosa* lysate and 97% positive wound samples contained $\geq 10^5$ bacteria per sample, the threshold value factoring in the infection risk (Supporting Information 10, Table S3).

Electrochemical Immunoassay. After optimization of the electrochemical method (Supporting Information 7), square wave voltammetry was successfully used to detect the bacteria in lysates (Figure 1A). Calibration curves were established by measuring the peak current after baseline correction (Figure 1B). The LOQ for EC-IA measurements

of lysates isolated by size exclusion and measured by sandwich assay was 10^4 bacteria per sample. The response was linear within the range 10^4 – 10^5 bacteria per sample ($R^2 > 0.99$). The EC-IA maintained the sensitivity of the optical high-affinity capture method using the same polyclonal antibodies (Figure 1B, compared to Figure S1C). Six clinical wound samples tested for the presence of *P. aeruginosa* with the pyocyanin reference assay strongly correlated ($R^2 > 0.97$) with the EC-IA method for *P. aeruginosa* with all pyocyanin positive sample (>0.8 ng/ μ L) correctly identified by EC-IA (10^4 cells/mL) (Supporting Information 11 and 12). The bias between the buffer and clinical samples was $<4\%$ and within the measurement error. The liberation solution for the –C–O– linkage did not suppress the electrochemical signal, unlike the reducing agents used to cleave –S–S– bonds.

Mass Spectrometric Immunoassay. The attachment of the polyclonal antibodies to nanoparticles (*E. coli* (EC), *S. aureus* (SA), *K. pneumoniae* (KP) and *P. aeruginosa* (PA)) was achieved using both C–O or S–S linkage chemistry and allowed unique RMLs (VV-5, AA-5, GL-5, IG-5, and ACS) for each nanoparticle. Figure 2A shows an example of collected mass spectrum with the relevant fragments identified. The signal intensities for the different RMLs (VV-5, AA-5, GL-5, and IG-5) and the internal standard (VI-5) are measured and the ratio RML/IS calculated. Calibration of the different RMLs using the internal standard that shares a common parent ion did allow for simultaneous multiplexed detection based on unique m/z fragments (Figure 2B). The selectivity of each SIERRA nanoparticles associated with the determined RML/IS was demonstrated by performing the MS-IA with bacterial samples at 10^5 cells/sample containing the corresponding bacteria ($n = 9$), other strains ($n = 3$), or no bacteria ($n = 3$) (detail of the detected MS signals and samples in Table S2). Figure 2C shows how, for each nanoparticle, the recovered cell counts could be calculated using the calibration curves. If the nanoparticles were exposed to a sample containing another stain or no bacteria, the signal would be in the range of the noise. Changing the –S–S– linkage to –C–O– linkage decreased the assay time by 30 min. The –C–O– linkage was stable at pH 7.0, but was immediately cleaved at pH < 5.5 , whereas

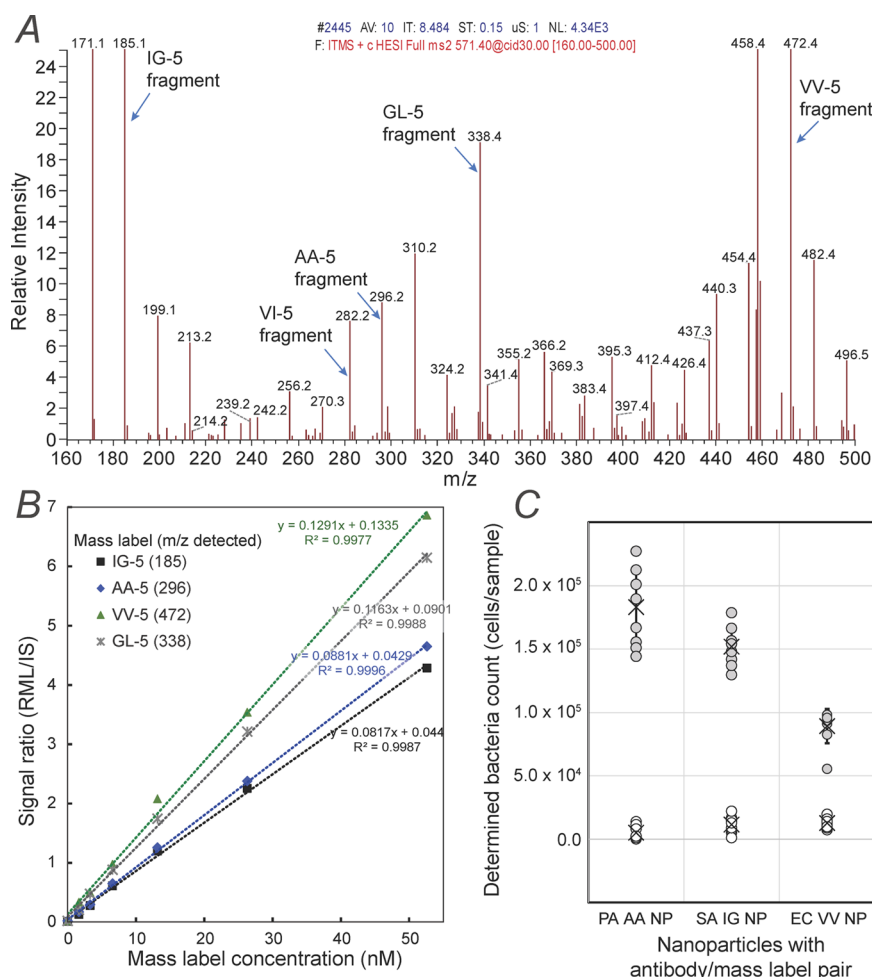


Figure 2. Bacterial MS-IA results. (A) Representative mass spectrum for a calibration standard containing AA-5, VV-5, IG-5, and GL-5 at 26.3 nM and internal standard VI-5 at 52.6 nM showing fragment mass for each label. (B) Average signal ratio for the released mass label (RML) to the internal standard (IS) plotted for four calibration solutions containing each of the RML separately. (C) Number of bacteria detected after sandwich immunoassay using the size-exclusion particle capture method is shown for three SIERRA nanoparticle (NP) mass label antibody pairs using lysate samples ($n = 9$, gray circles) containing the expected bacteria and samples ($n = 9$, empty circles) containing other or no bacteria.

the cleavage of $-S-S-$ linkage using TCEP took at least 30 min.

Flow cytometry of intact bacteria bound with SIERRA nanoparticles revealed that positively charged nanoparticles were binding to the bacterial membranes resulting in nonspecific binding to the bacteria, even in the absence of antibodies. We found that the attachment of PEG on 10% of the available nanoparticle sites eliminated the background binding. However, the number of RMLs that could be loaded per nanoparticle was reduced ($\sim 80\%$). Previously, we showed that nanoparticles containing $\sim 20\,000$ RMLs did not bind the membranes of eukaryotic cells (cancer cells).³⁷ Prokaryotic cells (bacteria cells) were considerably more likely to bind the loaded nanoparticle. The LOD was significantly higher than the LOD of 0.1 nM obtained previously for higher RML loading.³⁷

Genetic Analysis for the Identification and Quantitation of Bacteria. To confirm the presence of bacteria isolated by size-exclusion filtration, the 16S rRNA gene was amplified as previously described.³¹ An additional stretch of common sequence within the amplified region was selected as the probe for qPCR analysis using TaqMan chemistry to allow quantitation for bacteria cell count by qPCR. We also

used the TaqMan qPCR approach to test for the presence of *CTX-M* genes encoding enzymes that hydrolyze β -lactam antibiotics, the most widely used antibiotics in the world.^{38,39}

The probes for the 16S rRNA and *CTX-M* genes were labeled with different fluorophores for multiplex analysis.

To demonstrate that genetic analysis was compatible with the MS-IA analysis, synthetic urine was spiked with nonresistant and resistant *E. coli*, and lysates were collected for qPCR analysis after the size-exclusion particle capture method and the cleavage of RMLs for MS-IA. We found that synthetic oligonucleotides lacking 16S rRNA and *CTX-M* gene sequences were needed as blocking reagents for polycarbonate track-etched but not PVDF membranes. The *CTX-M* gene was present solely in the resistant *E. coli* strain, whereas the 16S rRNA gene was detected in both strains confirming the specificity of the qPCR assay (Figure 3A). This allowed the successful quantitation of 16S rRNA and *CTX-M* genes from *E. coli* cells in the range 10^2 – 10^5 per sample (Figure 3B). However, the ability to quantitation bacteria by qPCR was greatly reduced to over 10^7 cells when bacteria were isolated from 0.9 mL of urine (Figure 3C). Sample interference due to the presence of cell-free DNA impacted the qPCR background. This occurred whether using

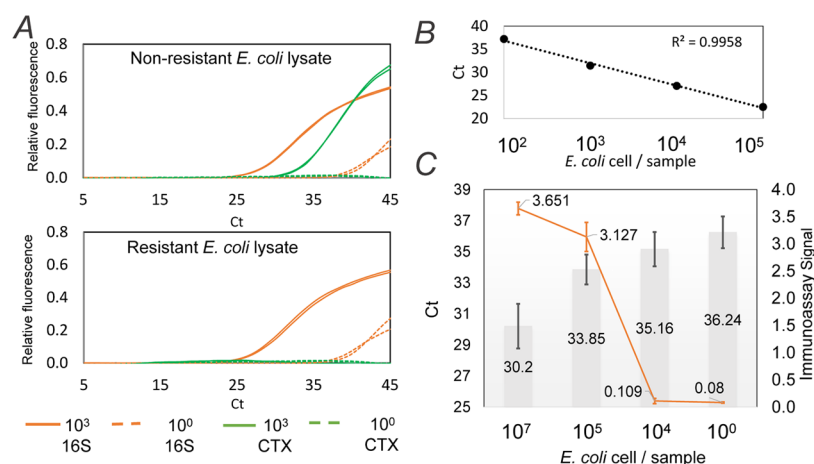


Figure 3. Bacterial DNA analysis after size-exclusion filtration. (A) TaqMan-based qPCR assays for 16S rRNA and CTX-M genes allowed for gene detection and quantitation after the extraction of *E. coli* DNA from the membrane: Presence of 16S rRNA in both strains and CTX-M genes only in the resistant strain confirmed the specificity of the assay. (B) Sensitivity of the qPCR method is shown for *E. coli* cells in buffer. (C) Sensitivities for *E. coli* cells isolated from urine by 16S DNA qPCR (left axis, results in columns) were more limited and not as sensitive as the immunoassay response (right axis, orange data points).

A		B		C					
S. aureus		P. aeruginosa		E. Coli					
Immunoassay		Immunoassay		Immunoassay					
Neg Pos		Neg Pos		Neg Pos					
Culture Neg	129	22	137	12	115	4			
Culture Pos	3	15	1	20	4	47			
TN	129	sens	83%	137	sens	95%	115	sens	92%
FN	3	spec	85%	1	spec	92%	4	spec	97%
FP	22	PPV	41%	12	PPV	63%	4	PPV	92%
TP	15	NPV	98%	20	NPV	99%	47	NPV	97%

D		E		F					
Bacteriuria		16S qPCR		CTX-M qPCR					
Immunoassay		Immunoassay		ESBL					
Neg Pos		Neg Pos		Neg Pos					
Culture Neg	66	13	17	40	203	16			
Culture Pos	7	83	14	157	1	8			
TN	129	sens	92%	17	sens	92%	203	sens	89%
FN	3	spec	84%	14	spec	30%	1	spec	93%
FP	22	PPV	86%	40	PPV	80%	16	PPV	33%
TP	15	NPV	90%	157	NPV	55%	8	NPV	100%

Figure 4. Clinical agreement. Agreement of immunoassays to matching organisms identified by culture ($>5 \times 10^4$ cell/mL) is shown for urine specimens ($n = 169$). Cultures containing *Enterococcus* spp. *E. faecalis*, *Streptococcus agalactiae*, *Lactobacillus* spp, *Proteus mirabilis*, *Candida albicans*, or no bacteria were considered negative. (E, F). Agreement of qPCR 16S as an indicator of bacteriuria or CTX-M qPCR as an indicator of extended-spectrum β -lactamase resistance (ESBL) is shown for urine specimens ($n = 222$) measured by culture.

standard DNA purification methods or using size-exclusion filtration isolation. By comparison, the immunoassay maintained 5×10^4 bacteria sensitivity for complex samples.

Clinical Sample Verification. As final proof of the method, the agreement of the immunoassay for *S. aureus*, *P. aeruginosa*, and *E. coli* were compared against culture using remnant deidentified patient urine samples ($n = 169$). The sensitivities for these immunoassays were 83, 95, and 92% for the prediction of *S. aureus*, *P. aeruginosa*, and *E. coli* or *K. pneumoniae* positive culture, respectively, while the specificities were 85, 92, and 97% (Figure 4A–C). The lower clinical sensitivity of the *S. aureus* immunoassay was predicted by the poor LOD due to higher variation in the background due to some antibodies binding to membranes. Typically, antibodies are further optimized by modifications to reduce such binding. Surprisingly, the *E. coli* immunoassay which was not suggested to bind *K. pneumoniae* in contrived testing did show a correlation in the case of clinical samples.

The overall agreement for bacteriuria far surpassed our previous studies with urine strips or immunochromatography strips.²⁶

Indication of bacteriuria by 16S qPCR after size-exclusion isolation and lysis was sensitive (92%) but very nonspecific (30%) with many false positives, in agreement to observed reduced LOQ expected from cell-free bacterial DNA circulating in the sample. The qPCR for any of the β -lactamase cefotaximase gene (CTX-M) after bacterial cell isolation and lysis was specific (93%) and sensitive (89%), as an indication of the presence of extended-spectrum β -lactamase resistance (ESBL) ($n = 9$). The increased specificity compared to 16S could be expected as any cell-free component of this gene would be less significant.

The new increased sensitivity ($>95\%$) of immunoassays without loss of specificity ($>92\%$) has not previously been achieved in POC. Using the fluidic principles of compatible methods for sample preparation and reagents solves the integration problems associated with a rapid concentration of

complex samples into a small reaction volume (20–150 μL) needed for immunoassays and selective cell capture.

The typical current practice for infection status consists of a collection with some POC reflex testing (i.e., subsequent tests only performed after initial screening test), and positive samples are sent to the laboratory for culture (10–24 h), followed by manual review for identification (0.5–6 h) done in parallel to susceptibility testing (4–10 h). The final results are typically expected in 3–5 days. Standard POC tests however have poor specificity for infection with a low positive predictive value (PPV), and at least one out of every two patients has a false-positive diagnosis without a confirmatory urine culture. The result of POC testing for infection is an increase in the number of unnecessary anti-infective therapies given to patients without infections and follow-up cultures. While the negative predictive value (NPV) is generally higher, false negatives are also a real issue and can lead patients with infection to never have samples sent for culture. The diagnostic platform presented here with fluidics and combined immunoassays allows for pathogen isolation within 5 min and identification in 15 min to 1 h before deciding on additional testing on a positive sample such as multiplexed or resistance gene assays (6 h). By rapidly identifying infections at the POC and allow confirmation of all pathogens in the laboratory, it would help reduce unnecessary anti-infective usage by correctly identifying infections sooner during treatment.

CONCLUSIONS

We set out to develop a sensitive MS-IA for multiplexed detection of bacteria based on nondestructive SIERRA technology, in a format which is compatible with the upstream analysis by EC-IA and downstream analysis of genetic markers from the same samples. We found a MS-IA method that was compatible for measuring bacterial lysis with EC-IA and DNA analysis by qPCR and demonstrate a new rapid release of mass labels at pH 5.2 using an ether linkage, which reduced the time to result. Both immunoassays achieved 10^5 bacteria sensitivity using a size-exclusion capture particle format. Our results show that the integration of EC-IA, MS-IA, and genetic analysis can work together as a platform technology to rapidly identify different bacterial species or even different strains in a sensitive and easily automated size-exclusion microtiter plate format that is suitable for life science applications.

ASSOCIATED CONTENT

Supporting Information

The Supporting Information is available free of charge at <https://pubs.acs.org/doi/10.1021/acs.analchem.0c00453>.

Additional experimental methods and results; microbiologic method for bacterial culturing; screen methods for bacterial polyclonal antibody reagents; SIERRA nanoparticle schematic, synthesis, and characterization; format of the 96-well fluidic filtration platform; size-exclusion isolation methods; EC *p*-aminophenol determination; MS–MS releasable mass labels determination; results of 16S sequencing; results for wound samples and method for pyocyanin; and calculation of LOD and LOQ (PDF)

AUTHOR INFORMATION

Corresponding Author

Frédérique Deiss – Department of Chemistry & Chemical Biology, Indiana University—Purdue University Indianapolis (IUPUI), Indianapolis, Indiana 46202, United States; orcid.org/0000-0002-8626-5370; Phone: (317) 278-5507; Email: fdeiss@iupui.edu

Authors

Michael Puglia – Bioanalytical Technologies, Indiana Biosciences Research Institute (IBRI), Indianapolis, Indiana 46202, United States

Tiyash Bose – Bioanalytical Technologies, Indiana Biosciences Research Institute (IBRI), Indianapolis, Indiana 46202, United States

Marco Tjioe – Bioanalytical Technologies, Indiana Biosciences Research Institute (IBRI), Indianapolis, Indiana 46202, United States

Dylan Frabutt – Bioanalytical Technologies, Indiana Biosciences Research Institute (IBRI), Indianapolis, Indiana 46202, United States

Zane Baird – Bioanalytical Technologies, Indiana Biosciences Research Institute (IBRI), Indianapolis, Indiana 46202, United States; orcid.org/0000-0001-5725-0375

Zehui Cao – Bioanalytical Technologies, Indiana Biosciences Research Institute (IBRI), Indianapolis, Indiana 46202, United States

Anna Vorsilak – Bioanalytical Technologies, Indiana Biosciences Research Institute (IBRI), Indianapolis, Indiana 46202, United States

Ian McLuckey – Bioanalytical Technologies, Indiana Biosciences Research Institute (IBRI), Indianapolis, Indiana 46202, United States

M. Regina Barron – Bioanalytical Technologies, Indiana Biosciences Research Institute (IBRI), Indianapolis, Indiana 46202, United States; Department of Chemistry & Chemical Biology, Indiana University—Purdue University Indianapolis (IUPUI), Indianapolis, Indiana 46202, United States

Monica Barron – Bioanalytical Technologies, Indiana Biosciences Research Institute (IBRI), Indianapolis, Indiana 46202, United States; Department of Chemistry & Chemical Biology, Indiana University—Purdue University Indianapolis (IUPUI), Indianapolis, Indiana 46202, United States

Gerald Denys – Division of Clinical Microbiology, Department of Pathology and Laboratory Medicine, IU Health Pathology Laboratory, Indiana University School of Medicine, Indianapolis, Indiana 46202, United States

Jessica Carpenter – Division of Clinical Microbiology, Department of Pathology and Laboratory Medicine, IU Health Pathology Laboratory, Indiana University School of Medicine, Indianapolis, Indiana 46202, United States

Amitava Das – Indiana Center for Regenerative Medicine and Engineering (ICRME), IU Health Comprehensive Wound Center, Department of Surgery, Indiana University School of Medicine, Indianapolis, Indiana 46202, United States

Karamjeet Kaur – Indiana Center for Regenerative Medicine and Engineering (ICRME), IU Health Comprehensive Wound Center, Department of Surgery, Indiana University School of Medicine, Indianapolis, Indiana 46202, United States

Sashwati Roy – Indiana Center for Regenerative Medicine and Engineering (ICRME), IU Health Comprehensive Wound Center, Department of Surgery, Indiana University School of Medicine, Indianapolis, Indiana 46202, United States

Chandan K. Sen – Indiana Center for Regenerative Medicine and Engineering (ICRME), IU Health Comprehensive Wound Center, Department of Surgery, Indiana University School of Medicine, Indianapolis, Indiana 46202, United States

Complete contact information is available at:
<https://pubs.acs.org/10.1021/acs.analchem.0c00453>

Author Contributions

M.P., Z.B., M.T., M.R.B., and I.M. contributed to nanoparticle design and SIERRA assay development; Z.C., A.V., and M.P. contributed to molecular assay design; M.J., D.F., and M.P. contributed to antibody selection; A.V. and M.P. contributed to microbiological standards; T.B., M.B., M.R.B., F.D., A.V., Z.C., and M.P. contributed to electrochemical assay development; and A.D., K.K., S.R., M.P., G.D., J.C., and C.K.S. contributed to clinical sampling and clinical direction.

Notes

The authors declare no competing financial interest.

ACKNOWLEDGMENTS

This project was supported by Disease Diagnostics INventors Challenge awards by Indiana CTSI to S.R., Z.B., M.P. and A.D., NIH R01NR015676 to C.K.S. and S.R., NIH R01DK125835 to C.K.S. and NIH R01DK114718 to S.R.

REFERENCES

- (1) U.S.Center for Disease Control and Prevention. *Antibiotic Resistance Threats in the United States, 2019*; U.S. Department of Health and Human Services, CDC: Atlanta, GA, 2019.
- (2) N. C. D. Risk Factor Collaboration. *Lancet* **2016**, *387*, 1513–1530.
- (3) Gregg, E. W.; Hora, I.; Benoit, S. R. *J. Am. Med. Assoc.* **2019**, *321*, 1867–1868.
- (4) Pavlou, S.; Lindsay, J.; Ingram, R.; Xu, H. P.; Chen, M. *BMC Immunol.* **2018**, *19*, No. 24.
- (5) Hulleigie, S.; Wootton, M.; Verheij, T. J. M.; Thomas-Jones, E.; Bates, J.; Hood, K.; Gal, M.; Francis, N. A.; Little, P.; Moore, M.; et al. *Fam. Pract.* **2017**, *34*, 392–399.
- (6) Lecube, A.; Pachon, G.; Petriz, J.; Hernandez, C.; Simo, R. *PLoS One* **2011**, *6*, No. e23366.
- (7) Raghav, A.; Khan, Z. A.; Labala, R. K.; Ahmad, J.; Noor, S.; Mishra, B. K. *Ther. Adv. Endocrinol. Metab.* **2018**, *9*, 29–31.
- (8) Alexiadou, K.; Doupis, J. *Diabetes Ther.* **2012**, *3*, No. 4.
- (9) Foxman, B. *DM, Dis.-Mon.* **2003**, *49*, 53–70.
- (10) Manoharan, A.; Winter, J. *Practitioner* **2010**, *254*, 25–28.
- (11) Price, T. K.; Dune, T.; Evann, E. E.; Thomas-White, K. J.; Kliethermes, S.; Brincat, C.; Brubake, L.; Wolfe, A. J.; Mueller, E. R.; Schreckenberger, P. C. *J. Clin. Microbiol.* **2016**, *54*, 1216–1222.
- (12) Opota, O.; et al. *Clin. Microbiol. Infect.* **2015**, *21*, 313–322.
- (13) Wolcott, R.; Dowd, S. *Plast. Reconstr. Surg.* **2011**, *127*, 28S–35S.
- (14) Ganesh, K.; Das, A.; Dickerson, R.; Khanna, S.; Parinandi, N. L.; Gordillo, G. M.; Sen, C. K.; Roy, S. *J. Immunol.* **2012**, *189*, 2563–2573.
- (15) Das, A.; Ghatak, S.; Sinha, M.; Chaffee, S.; Ahmed, N. S.; Parinandi, N. L.; Wohleb, E. S.; Sheridan, J. F.; Sen, C. K.; Roy, S. *J. Immunol.* **2016**, *196*, S089–S100.
- (16) Reyes, E. A.; Bale, M. J.; Cannon, W. H.; Matsen, J. M. *J. Clin. Microbiol.* **1981**, *13*, 456–458.
- (17) Kushwaha, M.; Jain, S. K.; Sharma, N.; Abrol, V.; Jaglan, S.; Vishwakarma, R. A. *ACS Chem. Biol.* **2018**, *13*, 657–665.
- (18) DiGiandomenico, A.; Sellman, B. R. *Curr. Opin. Microbiol.* **2015**, *27*, 78–85.
- (19) Dryla, A.; Prustomersky, S.; Gelbmann, D.; Hanner, M.; Bettinger, E.; Kocsis, B.; Kustos, T.; Henics, T.; Meinke, A.; Nagy, E. *Clin. Diagn. Lab. Immunol.* **2005**, *12*, 387–398.
- (20) Knirel, Y. A. *Crit. Rev. Microbiol.* **1990**, *17*, 273–304.
- (21) Pennini, M. E.; De Marco, A.; Pelletier, M.; Bonnell, J.; Cvitkovic, R.; Beltramello, M.; Camerani, E.; Bianchi, S.; Zatta, F.; Zhao, W.; et al. *Nat. Commun.* **2017**, *8*, No. 1991.
- (22) Dreisbach, A.; van Dijk, J. M.; Buist, G. *Proteomics* **2011**, *11*, 3154–3168.
- (23) Crestani, S.; Leitolis, A.; Lima, L. F. O.; Krieger, M. A.; Foti, L. *J. Immunol. Methods* **2016**, *435*, 17–26.
- (24) Marolda, C. L.; Lahiry, P.; Vinés, E.; Saldías, S.; Valvano, M. A. *Methods Mol. Biol.* **2006**, *347*, 237–252.
- (25) Moor, K.; Fadlallah, J.; Toska, A.; Sterlin, D.; Balmer, M. L.; Macpherson, A. J.; Gorochov, G.; Larsen, M.; Slack, E. *Nat. Protoc.* **2016**, *11*, 1531–1553.
- (26) Pugia, M. J.; Sommer, R. G.; Kuo, H. H.; Corey, P. F.; Gopual, D. L.; Lott, J. A. *Clin. Chem. Lab. Med.* **2004**, *42*, 340–346.
- (27) Coenye, T.; Vandamme, P. *FEMS Microbiol. Lett.* **2003**, *228*, 45–49.
- (28) Weisburg, W. G.; Barns, S. M.; Pelletier, D. A.; Lane, D. J. *J. Bacteriol.* **1991**, *173*, 697–703.
- (29) McDonald, M.; Kameh, D.; Johnson, M. E.; Johansen, T. E. B.; Albala, D.; Mouraviev, V. *Rev. Urol.* **2017**, *19*, 213–220.
- (30) Whiteside, S. A.; Razvi, H.; Dave, S.; Reid, G.; Burton, J. P. *Nat. Rev. Urol.* **2015**, *12*, 81–90.
- (31) Klindworth, A.; Pruesse, E.; Schweer, T.; Peplies, J.; Quast, C.; Horn, M.; Glöckner, F. O. *Nucleic Acids Res.* **2013**, *41*, No. e1.
- (32) Pugia, M. J.; Blankenstein, G.; Peters, R. P.; Profitt, J. A.; Kadel, K.; Willms, T.; Sommer, R.; Kuo, H. H.; Schulman, L. S. *Clin. Chem.* **2005**, *51*, 1923–1932.
- (33) Magbanua, M. J. M.; Pugia, M. J.; Lee, J. S.; Jabon, M.; Wang, V.; Gubens, M.; Marfurt, K.; Pence, J.; Sidhu, H.; Uzgiris, A.; Rugo, H. S.; Parks, J. *PLoS One* **2015**, *10*, No. e0141166.
- (34) Wang, J.; Profitt, J. A.; Pugia, M. J.; Suni, I. I. *Anal. Chem.* **2006**, *78*, 1769–1773.
- (35) Basu, M.; Seggerson, S.; Henshaw, J.; Jiang, J.; del A Cordona, R.; Lefave, C.; Boyle, P. J.; Miller, A.; Pugia, M.; Basu, S. *Glycoconj. J.* **2004**, *21*, 487–496.
- (36) Olanrewaju, A. O.; Ng, A.; DeCorwin-Martin, P.; Robillard, A.; Juncker, D. *Anal. Chem.* **2017**, *89*, 6846–6853.
- (37) Baird, Z.; Cao, Z.; Barron, M. R.; Vorsilak, A.; Deiss, F.; Pugia, M. J. *Anal. Chem.* **2019**, *91*, 2028–2034.
- (38) Cantón, R.; González-Alba, J. M.; Galán, J. C. *Front. Microbiol.* **2012**, *3*, No. 110.
- (39) Naas, T.; Oxacelay, C.; Nordmann, P. *Antimicrob. Agents Chemother.* **2007**, *51*, 223–230.